Supporting Information

A Commercial Conducting Polymer as Both Binder and Conductive Additive for Silicon Nanoparticle-Based Lithium-Ion Battery Negative Electrodes

Thomas M Higgins,[1,2*] Sang-Hoon Park,[1,3*] Paul J King,[1,4] Chuanfang (John) Zhang,[1,3] Niall McEvoy,[1,3] Nina C. Berner,[1,3] Dermot Daly,[1,2] , Aleksey Shmeliov[1,3], Umar Khan,[1,2] Georg Duesberg,[1,3] Valeria Nicolosi,[1,3**] Jonathan N Coleman,[1,2**]

[1] *Centre for Research on Adaptive Nanostructures and Nanodevices (CRANN) & Advanced Materials Bio-Engineering Research Centre (AMBER), Trinity College Dublin, Dublin 2, Ireland.*

[2]*School of Physics, Trinity College Dublin, Dublin 2, Ireland*

[3]*School of Chemistry, Trinity College Dublin, Dublin 2, Ireland*

[4]*Efficient Energy Transfer Department, Bell Labs Research, Nokia, Blanchardstown Business & Technology Park, Snugborough Road, Dublin 15 Ireland*

*These authors contributed equally

** *nicolov@tcd.ie, colemaj@tcd.ie*

KEYWORDS: anode, battery, binder, conducting polymer, conducting additive, negative electrode, PEDOT:PSS, silicon.

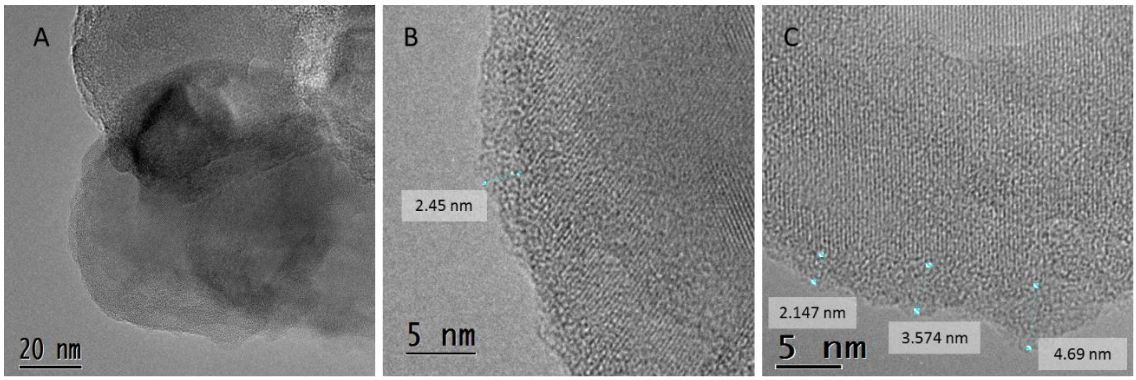

Figure S1. (a) Low magnification TEM image of the SiNPs used in this study. (b-c) High magnification TEM image of the SiNP surface at different positions. The high magnification images indicate that the particles are crystalline with a distinguishable oxide layer with thickness between 2 and 5 nm.

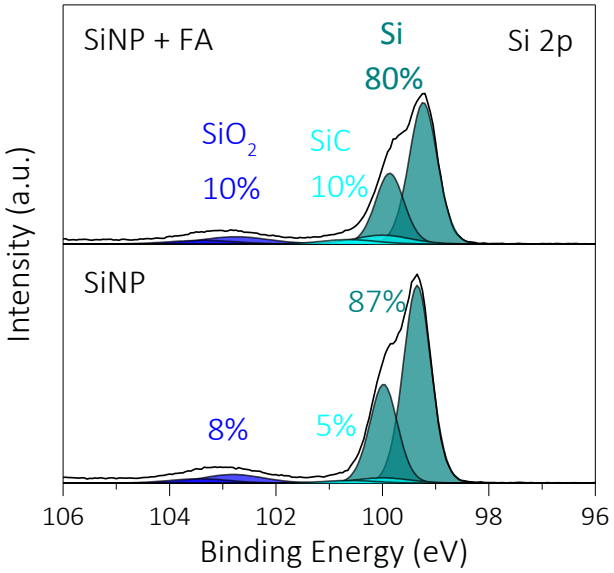

Figure S2. XPS Si 2p core-level spectra of the SiNPs without (lower spectrum) and with exposure to formic acid (upper spectrum). Both samples exhibit a major component at a binding energy of 99.3 eV, which is associated with elemental silicon. An additional component at ~101 eV indicates that roughly 10% of the SiNPs' atoms are oxidized in both cases. The only significant difference between the SiNPs with and without the FA treatment is the increased amount of silicon carbide formation, as indicated by the component at 100 eV.

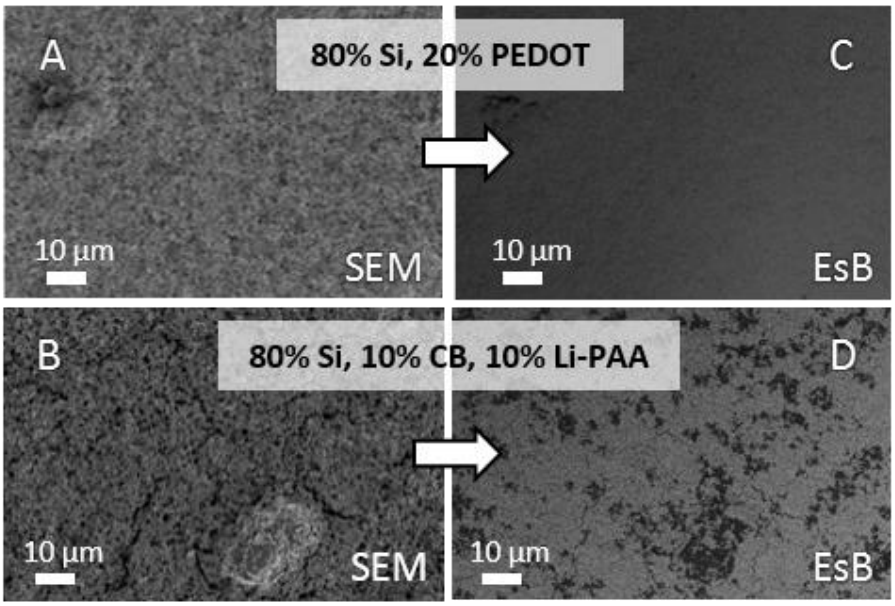

Figure S3. Wide view SEM (a & b) with energy-selective backscatter (EsB) mapping images of the corresponding areas (c & d) for the PEDOT:PSS/SiNP and CB/Li-PAA/SiNP electrodes, respectively.

Table S1. Sample preparation conditions for 20% PEDOT:PSS/SiNP electrode with different FA loadings up to 20 % (relative to the volume of PEDOT:PSS solution).

Sample condition	PEDOT:PSS content	PEDOT:PSS solution	SiNP powder	FA
0 % FA addition	20 wt% PEDOT:PSS	1 ml (11 mg PEDOT:PSS)	99 mg	-
1 % FA addition	20 wt% PEDOT:PSS	1 ml (11 mg PEDOT:PSS)	99 mg	0.01 ml
2 % FA addition	20 wt% PEDOT:PSS	1 ml (11 mg PEDOT:PSS)	99 mg	0.02 ml
5 % FA addition	20 wt% PEDOT:PSS	1 ml (11 mg PEDOT:PSS)	99 mg	0.05 ml
10 % FA addition	20 wt% PEDOT:PSS	1 ml (11 mg PEDOT:PSS)	99 mg	0.10 ml
15 % FA addition	20 wt% PEDOT:PSS	1 ml (11 mg PEDOT:PSS)	99 mg	0.15 ml
20 % FA addition	20 wt% PEDOT:PSS	1 ml (11 mg PEDOT:PSS)	99 mg	0.20 ml

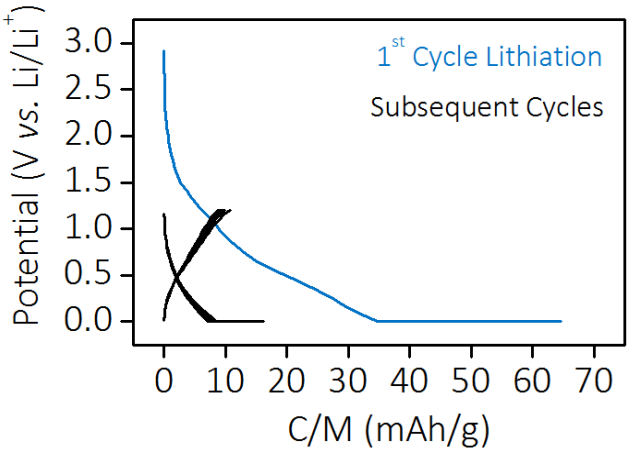

Figure S4. Lithiation/delithiation profiles for a PEDOT:PSS-only electrode during repeated cycling. The charge and discharge protocol used is the same as for the composite electrodes (see Methods).

Table S2. 1st cycle capacities for 20% PEDOT:PSS/SiNP electrodes with different FA additions.

Sample name	1st Lithiation capacity (mAh/g)	1st Delithiation capacity (mAh/g)	1st Irreversible capacity (mAh/g)
0% FA addition	3325	2389	936
5% FA addition	3436	2635	801
10% FA addition	3685	2854	831

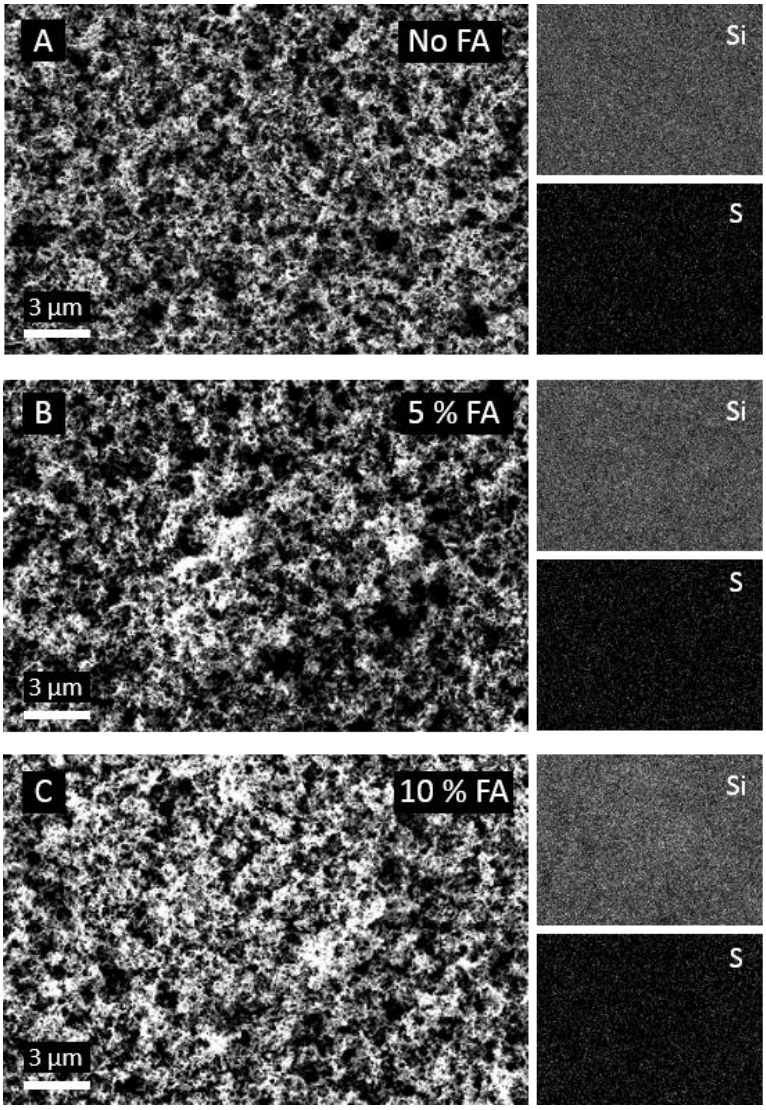

Figure S5. SEM and EDX maps for silicon and sulfur atoms for a 20 wt% PEDOT:PSS/SiNP composite film prepared with FA (a) as well as equivalent samples that have been exposed to 5% (b) and 10% FA (c).

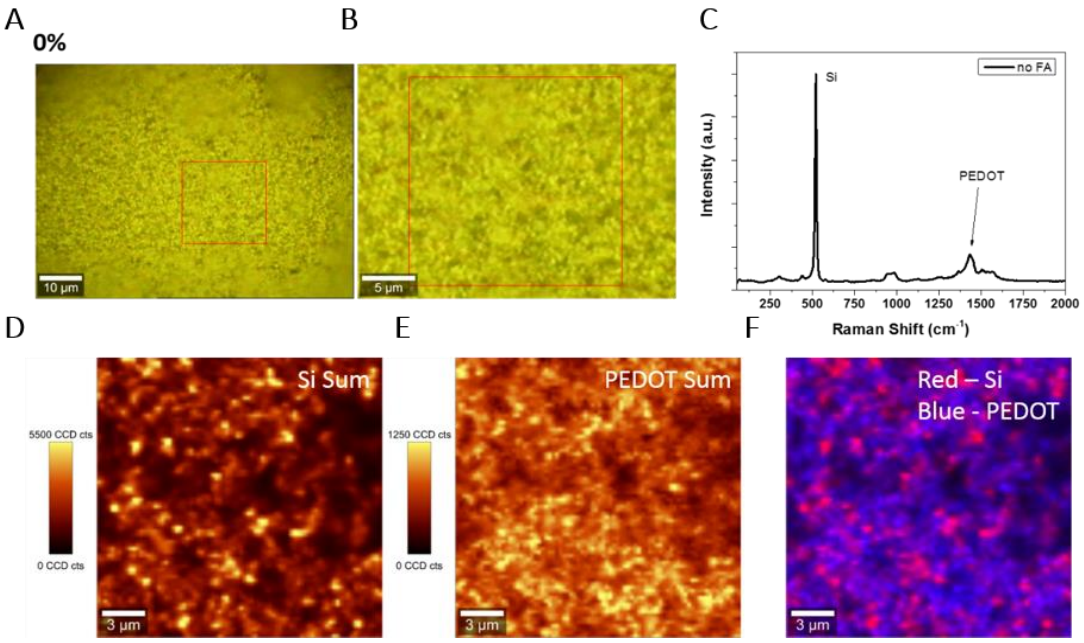

Figure S6. (a, b) Optical microscopy images of PEDOT:PSS/SiNP samples prepred without FA. The area over which Raman maps were acquired is marked in red. (c) Average Raman spectrum extracted from mapped region. (d) Raman map of silicon peak sum (~520 cm^{-1}). (e) Raman map of the symmetric stretching mode of the aromatic C=C band in PEDOT (~1435 cm^{-1}). (f) Overlaid map of silicon and PEDOT sum showing good mixing.

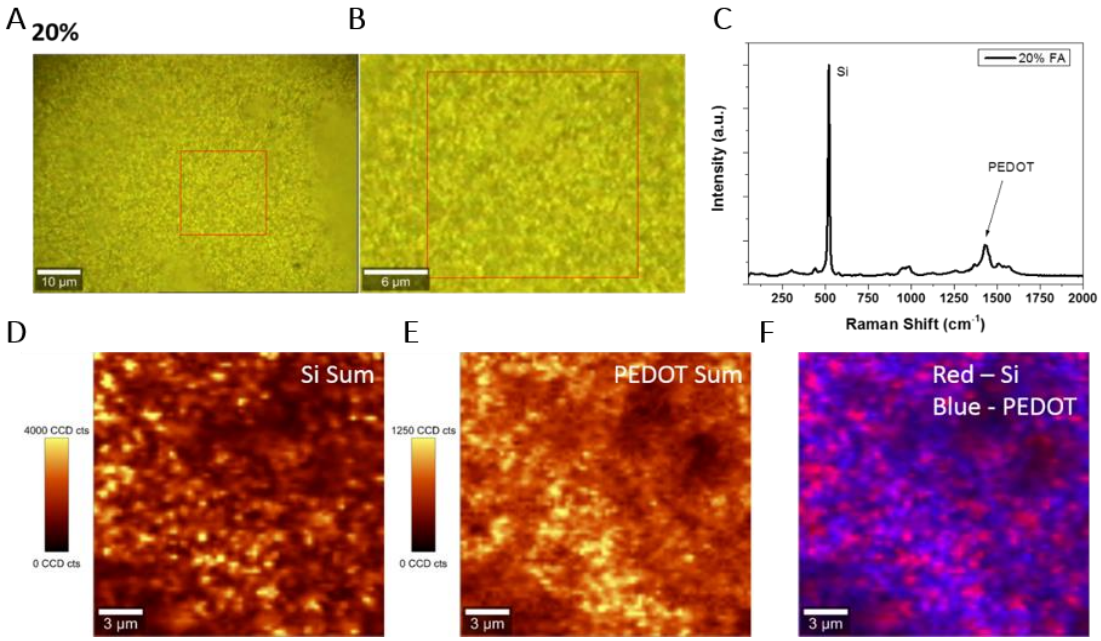

Figure S7. (a, b) Optical microscopy images of PEDOT:PSS/SiNP sample prepared with 20% FA. The area over which Raman maps were acquired is marked in red. (c) Average Raman spectrum extracted from mapped region. (d) Raman map of silicon peak sum (~520 cm^{-1}) (e) Raman map of the symmetric stretching mode of the aromatic C=C band in PEDOT (~1435 cm^{-1}). (f) Overlaid map of silicon and PEDOT sum showing good mixing.

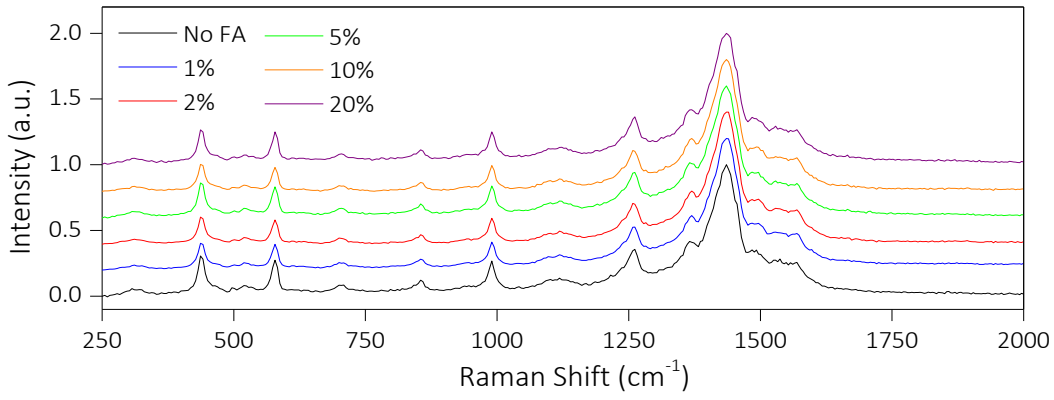

Figure S8. Average Raman spectra for pure PEDOT:PSS samples samples with different FA loading fractions normalized in intensity to the peak at @ 1435 cm^{-1}. All samples show a characteristic PEDOT:PSS signal with no change discernible change in peak position or relative intensities seen for different samples.

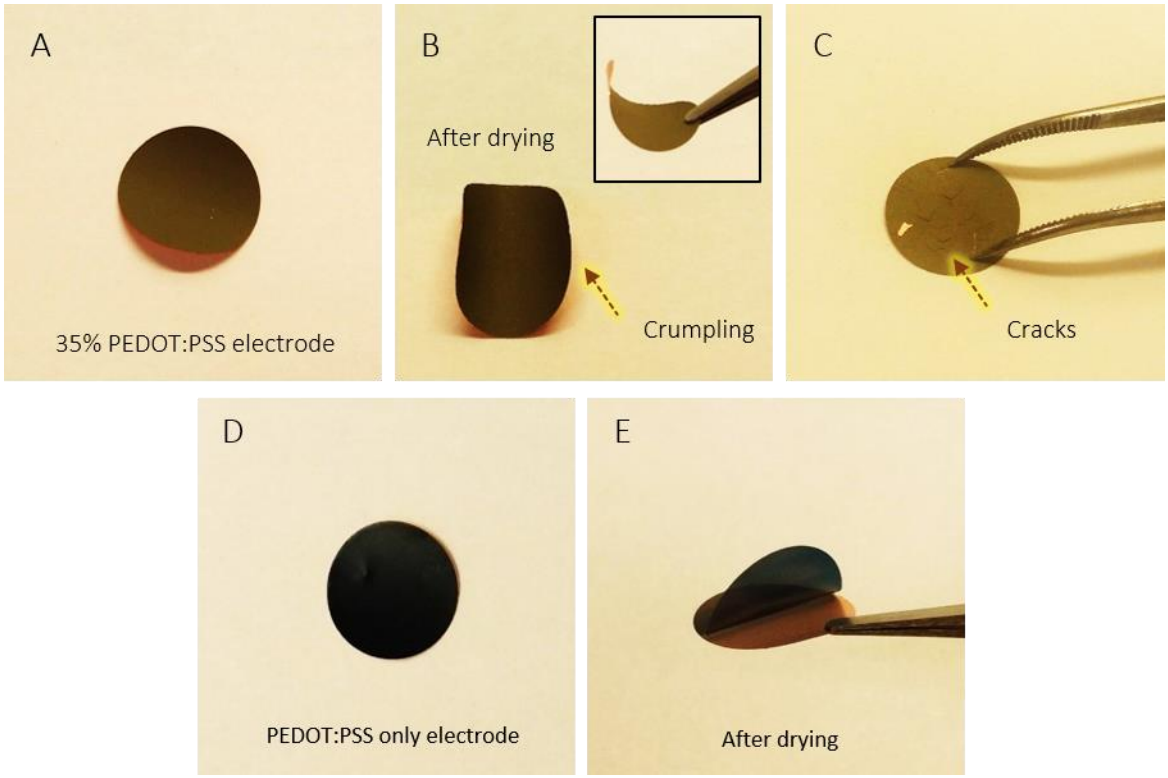

Figure S9. Photographic images of (a-c) 35 wt % PEDOT:PSS/SiNP electrode and (d-e) PEDOT:PSS electrode indicating cracking and mechanical adherence issue. The 35 wt % PEDOT:PSS/SiNP electrode was highly crumpled after the vacuum drying process (a-b) then cracked during flattening (c). This could be possible due to the relatively higher content of PEDOT:PSS; the PEDOT:PSS coated onto Cu foil can be easily peeled off from the substrate (d and e).

Table S3. Sample preparation conditions for the different PEDOT:PSS contents.

PEDOT:PSS content	Avg. mass loading (mg/cm^2)	Avg. thickness (um)	Avg. electrode density (g/cm^3)
5 wt % PEDOT:PSS	1.191	26.5	0.449
10 wt % PEDOT:PSS	1.085	21	0.517
15 wt % PEDOT:PSS	1.137	20.5	0.555
20 wt % PEDOT:PSS	1.016	17.5	0.581
25 wt % PEDOT:PSS	0.991	16.5	0.601
30 wt % PEDOT:PSS	1.167	19	0.614

Porosity Calculation:

$$\phi = \frac{V_{free}}{V_{total}} = \frac{V_{Total} - (V_{Si} + V_{PEDOT})}{V_{total}} = \frac{V_{total} - \left[\left(\frac{M_{Si}}{\rho_{Si,bulk}}\right) + \left(\frac{M_{PEDOT}}{\rho_{PEDOT,bulk}}\right)\right]}{V_{total}}$$

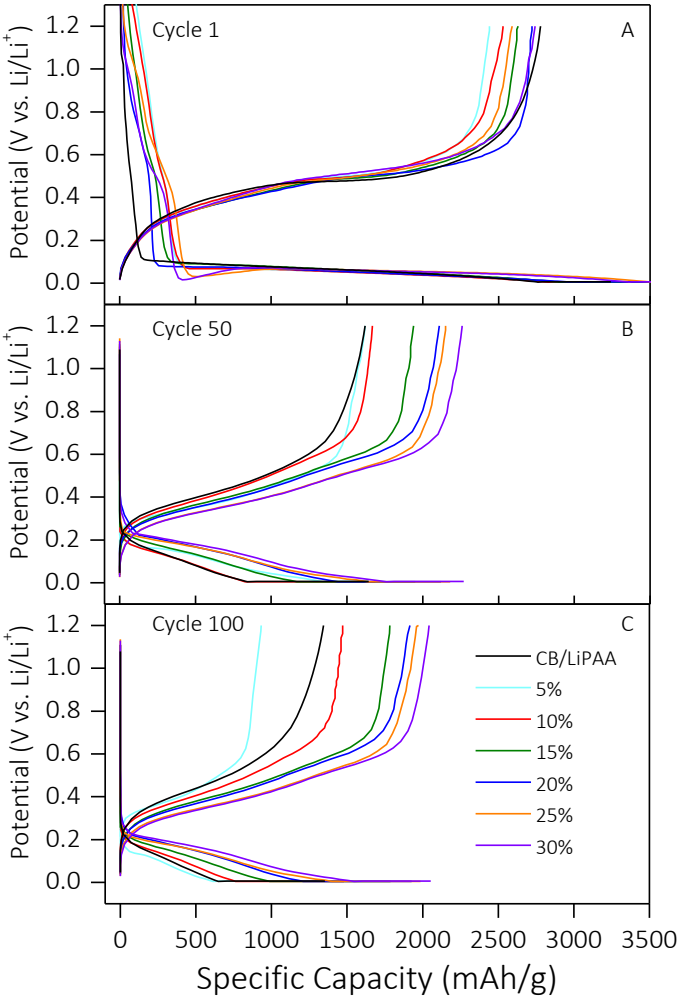

Figure S10. Lithiation/delithiation profiles for the Li-PAA/CB/Si tri-component electrode and the SiNP:PEDOT:PSS bi- component electrodes at the (a) 1st, (b) 50th, and (c) 100th cycles. Here we used CC-CV lithiation and following CC delithiation mode instead of conventional CC lithiation/delithiation mode. At the initial cycle (a) all the electrodes were first lithiated at 1000 mA/g (0.28 C-rate) and held at 0.005 V until the current decayed to 100 mA/g. Following this the electrodes were delithiated at 1000 mA/g until a 1.2 V cutoff was reached. After initial cycle, the electrodes were cycled at the twice faster condition (CC lithiation of 2000 mA/g (0.56 C-rate), CV until 200 mA/g, and following CC delithiation of 2000 mA/g) within the same potential windows (1.2 ~ 0.005 V).

Table S4. Electrode information for 20% PEDOT:PSS electrodes with various thickness.

Sample name	Mass loading (mg/cm^2)	Thickness (um)	Density (g/cm^3)
20 wt% PEDOT:PSS – 0.4 mg	0.438	7.5	0.584
20 wt% PEDOT:PSS – 0.8 mg	0.788	14	0.563
20 wt% PEDOT:PSS – 1.0 mg	1.016	17.5	0.581
20 wt% PEDOT:PSS – 1.5 mg	1.494	26	0.575

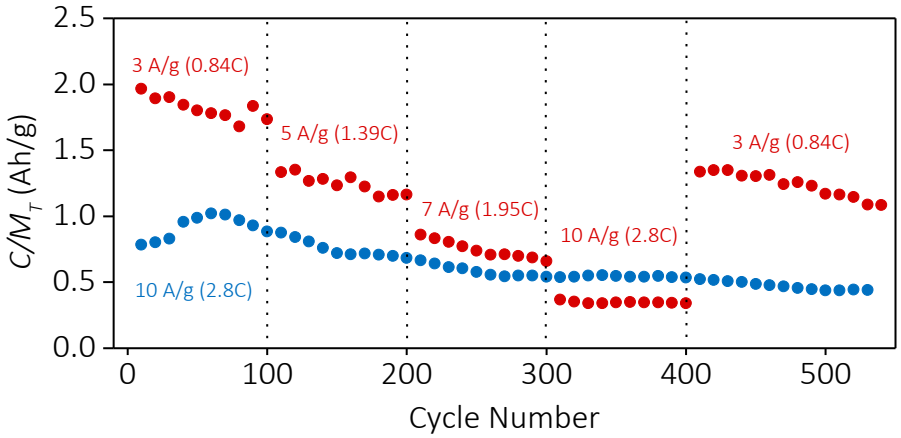

Figure S11. Specific capacity of a 20 wt % PEDOT:PSS/SiNP samples cycled over a longer duration (over 500th cycles) at constant current density of 10 A/g (2.8C) or different current densities from 3 A/g (0.84C) to 10 A/g (2.8C).

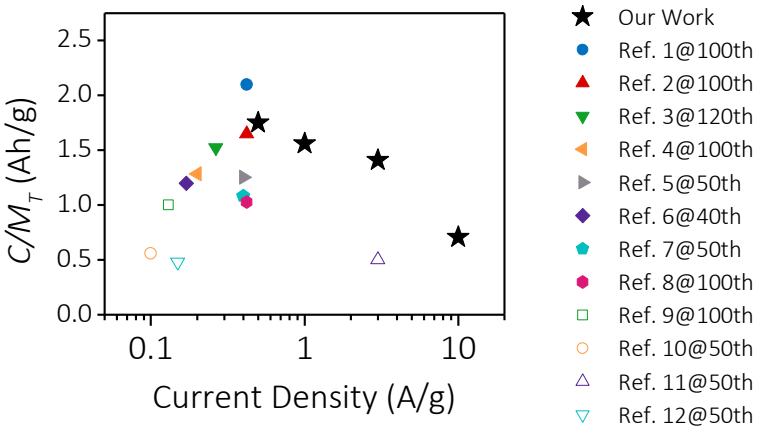

Figure S12. Total electrode normalized capacity as a function of current density for a 20 wt % PEDOT:PSS/SiNP film with *M/A*=1.0 mg/cm^2 at various current densities. Various literature data are also shown for comparison. See Table S5 for corresponding references (note all of these are from the larger *M/A* category).

Table S5. Comparison of the electrochemical performances for Si electrodes fabricated by novel binder system with commercial SiNP.

Type of binder	Electrode composition	Electrode mass loading	Electrode performance	Specific capacity normalized to total electrode	Ref.
High electrode loading mass over 1 mg/cm^2					
PEDOT:PSS conducting polymer	**Si : PEDOT:PSS = 80 : 20**	**0.4~1.5 mg/cm^2**	**1927 mAh/g @ 2 A/g, 100th** **2426 mAh/g @ 0.5 A/g, 50th** **2186 mAh/g @ 0.5 A/g,100th**	**1547 mAh/g** **1941 mAh/g** **1749 mAh/g**	**Our work**
Ca-Alginate binder	Si : Ca-Alginate : CB 70 : 15 : 15	1.1 mg/cm^2	~3000 mAh/g @ 0.42 A/g, 100th 2522 mAh/g @ 0.42 A/g, 500th	2100 mAh/g 1766 mAh/g	1
PAA/PANI IPN conducting polymer	Si: PAA/PANI IPN = 60 : 40	~ 1 mg/cm^2	~ 2750 mAh/g @ 0.42 A/g, 100th 2205 mAh/g @ 0.42 A/g, 300th	1650 mAh/g 1323 mAh/g	2
Self-healing binder	Si : CB : self-healing binder = 63.3 : 3.3 : 33.3	0.1~1.6 mg/cm^2	2407 mAh/g @ 0.265 A/g, then 0.088 A/g, 120th	1524 mAh/g	3
PEDOT:PSS conducting agent + CMC binder	Si : CB: PEDOT:PSS : CMC = 70 : 10 : 10 : 10	~ 1 mg/cm^2	1834 mAh/g @ 0.2 A/g, 100th	1284 mAh/g	4
SPEEK-PSI-Li binder	Si : CB : SPEEK-PSI-Li 60 : 20 : 20	~ 1.2 mg/cm^2	2090 mAh/g @ 0.4 A/g, 50th	1254 mAh/g	5
PPyE conducting polymer	Si: PPyE = 66.6 : 33.3	1.34 mg/cm^2 (0.15~0.3 mg/cm^2)	~1800 mAh/g @ 0.17 A/g, 40th (~2300 mAh/g @ 0.42 A/g, 180th)	1200 mAh/g (1532 mAh/g)	6
PAA-PVA gel polymer binder	Si : CB : PAA-PVA binder = 60 : 20 : 20	2.4 mg/cm^2	~1800 mAh/g @ 4 A/g, 50th	1080 mAh/g	7
CNT and PEDOT:PSS	Si : CNT/PEDOT = 57 : 43	~ 2 mg/cm^2	1802 mAh/g @ 0.42 A/g, 100th	1027 mAh/g	8
CMC	Si : CB : CMC = 33: 33: 33	2 .26 ~ 2.83 mg/cm^2	~3000 mAh/g @ ~0.13 A/g, 100th	1000 mAh/g	9
PAA	SiO : CB : PAA = 80 : 10 : 10	0.89 ~ 1.7 mg/cm^2	~700 mAh/g @ 0.1 A/g, 50th	560 mAh/g	10
Meldrum's acid incorporated polymer	Si : CB : binder = 60 : 20 : 20	0.9 mg/cm^2 for Si	~ 500 mAh/g (normalized on total electrode mass) @ 3 A/g, 50th	~ 500 mAh/g	11
PVDF	Si : CB : PVDF = 80 : 12 : 8	2.6 mg/cm^2	~ 600 mAh/g @ 0.15 A/g, 50th	480 mAh/g	12
Low electrode loading mass below 1 mg/cm^2					
PEEM conducting polymer	Si: PEEM = 66.6 : 33.3	~0.2 mg/cm^2	~3000 mAh/g @ 0.375 A/g, 50th	1998 mAh/g	13
PPQ conducting polymer	Si:PPQ = 70 : 30	~0.8 mg/cm^2 (0.55 mg/cm^2 for Si)	2823 mAh/g @ 0.358 A/g, 50th	1976 mAh/g	14
PFFOMB conducting polymer	Si: PFFOMB = 66.6 : 33.3	~0.3 mg/cm^2	~2400 mAh/g @ 0.42 A/g, 100th ~2100 mAh/g @ 0.42 A/g, 650th	1598 mAh/g 1400 mAh/g	15
PANi conducting polymer	Si:PANi = 75 : 25	0.3~0.4 mg/cm^2	~2100 mAh/g @ 0.3 A/g, 70th ~1200 mAh/g @ 1 A/g, 1000th	1575 mAh/g 900 mAh/g	16
Mussel-inspired binder	Si : CB : mussel-inspired binder = 60 : 20 : 20	0.2~0.3 mg/cm^2	~2500 mAh/g @ 2.1 A/g, 150th ~2000 mAh/g @ 2.1 A/g, 400th	1500 mAh/g 1200 mAh/g	17
Hyperbranched β-Cyclodextrin Polymer	Si : β-CDp : CB = 60 : 20 : 20	0.3~0.6 mg/cm^2 for Si	~ 1500 mAh/g (normalized on total electrode mass) @ 4.2 A/g 100th	~ 1500 mAh/g	18
Native xanthan gum binder	Si : CB : gum binder = 60 : 20 : 20	~ 0.3 mg/cm^2	~2400 mAh/g @ 3.5 A/g, 100th 2150 mAh/g @ 3.5 A/g, 200th	1440 mAh/g 1290 mAh/g	19
Arabic gum binder	Si : CB : arabic binder 50 : 25 : 25	0.3 mg/cm^2 for Si	2708 mAh/g @ 0.42 A/g, 100th	1354 mAh/g	20
PFM binder	Si : CB : PFM = 50 : 20 : 30	0.16 ~ 0.23 mg/cm^2	~2500 mAh/g @ 0.17 A/g, 30th	1200 mAh/g @ 30th	21

Unknown electrode loading mass					
PAI binder	Si : CB : PAI = 84: 6: 10	Unknown	~1700 mAh/g @ 0.42 A/g, 20th	1428 mAh/g	22
c-PAA-CMC binder	Si : CB : c-PAA-CMC = 60 : 20 : 20	Unknown	~ 2000 mAh/g @ 0.3 A/g, 100th	1200 mAh/g	23
Alginate binder	Si : CB : alginate binder = 63.75 : 21.25 : 15	Unknown	1700 mAh/g @ 4.2 A/g, 100th	1084 mAh/g	24
Alginate binder	SiC : CB : alginate binder = 53 : 18 : 29	Unknown	1822 mAh/g @ 0.42 A/g, 120th	966 mAh/g	25
PAA binder	Si : CB : PAA = 43 : 42 : 15	Unknown	~2000 mAh/g @ 2.1 A/g, 100th	860 mAh/g	26
PAA-co-PVA	Si : PAA-c0-PVA : CB = 60 : 20 : 20	Unknown	1250 mAh/g @ 0.2 A/g, 80th	750 mAh/g	27
Na-CMC binder	Si : CB : Na-CMC = 40: 40: 20	Unknown	~1000 mAh/g @ 2.1 A/g, 100th	400 mAh/g	28

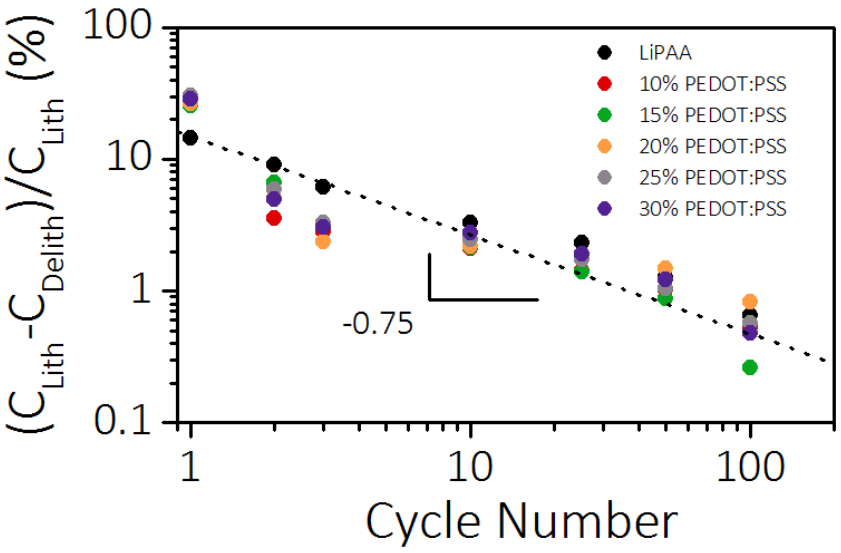

Figure S13. $(C_{Lith} - C_{Delith})/C_{Lith}$ (Coulombic inefficiency) vs. cycle number.

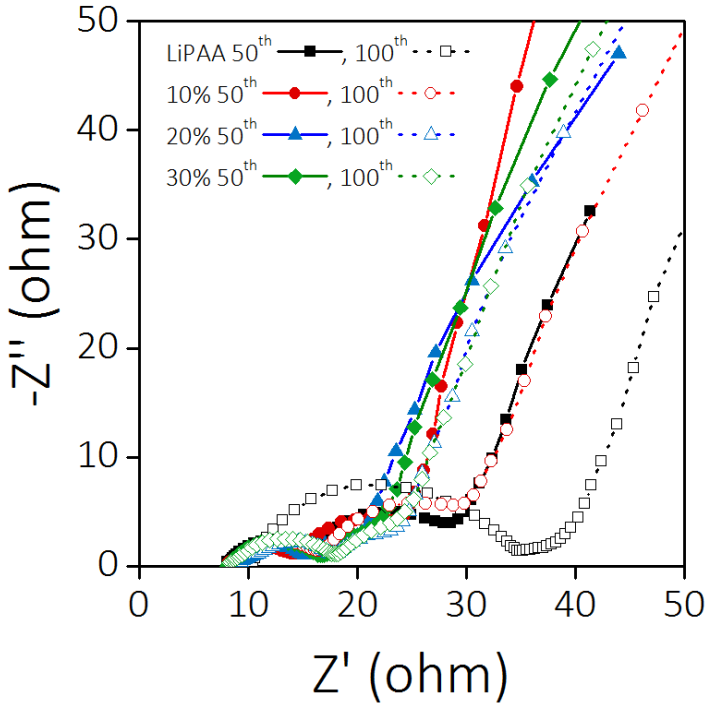

Figure S14. Nyquist plots for SiNP/CB/Li-PAA electrode and SiNP/PEDOT:PSS electrodes at 50^{th} and 100^{th} cycles.

Reference

1. Zhang, L.; Zhang, L. Y.; Chai, L. L.; Xue, P.; Hao, W. W.; Zheng, H. H., A Coordinatively Cross-Linked Polymeric Network as a Functional Binder for High-Performance Silicon Submicro-Particle Anodes in Lithium-Ion Batteries. *J Mater Chem A* **2014,** 2, 19036-19045.
2. Yu, X. H.; Yang, H. Y.; Meng, H. W.; Sun, Y. L.; Zheng, J.; Ma, D. Q.; Xu, X. H., Three-Dimensional Conductive Gel Network as an Effective Binder for High-Performance Si Electrodes in Lithium-Ion Batteries. *Acs Appl Mater Inter* **2015,** 7, 15961-15967.
3. Chen, Z.; Wang, C.; Lopez, J.; Lu, Z. D.; Cui, Y.; Bao, Z. A., High-Areal-Capacity Silicon Electrodes with Low-Cost Silicon Particles Based on Spatial Control of Self-Healing Binder. *Adv Energy Mater* **2015,** 5.
4. Shao, D.; Zhong, H. X.; Zhang, L. Z., Water-Soluble Conductive Composite Binder Containing Pedot: Pss as Conduction Promoting Agent for Si Anode of Lithium-Ion Batteries. *Chemelectrochem* **2014,** 1, 1679-1687.
5. Qin, D. J.; Xue, L. X.; Du, B.; Wang, J.; Nie, F.; Wen, L. L., Flexible Fluorine Containing Ionic Binders to Mitigate the Negative Impact Caused by the Drastic Volume Fluctuation from Silicon Nano-Particles in High Capacity Anodes of Lithium-Ion Batteries. *J Mater Chem A* **2015,** 3, 10928-10934.
6. Park, S. J.; Zhao, H.; Ai, G.; Wang, C.; Song, X. Y.; Yuca, N.; Battaglia, V. S.; Yang, W. L.; Liu, G., Side-Chain Conducting and Phase-Separated Polymeric Binders for High-Performance Silicon Anodes in Lithium-Ion Batteries. *J Am Chem Soc* **2015,** 137, 2565-2571.
7. Song, J. X.; Zhou, M. J.; Yi, R.; Xu, T.; Gordin, M. L.; Tang, D. H.; Yu, Z. X.; Regula, M.; Wang, D. H., Interpenetrated Gel Polymer Binder for High-Performance Silicon Anodes in Lithium-Ion Batteries. *Adv Funct Mater* **2014,** 24, 5904-5910.
8. Chen, Z.; To, J. W. F.; Wang, C.; Lu, Z. D.; Liu, N.; Chortos, A.; Pan, L. J.; Wei, F.; Cui, Y.; Bao, Z. N., A Three-Dimensionally Interconnected Carbon Nanotube-Conducting Polymer Hydrogel Network for High-Performance Flexible Battery Electrodes. *Adv Energy Mater* **2014,** 4.
9. Bridel, J. S.; Azaïs, T.; Morcrette, M.; Tarascon, J. M.; Larcher, D., Key Parameters Governing the Reversibility of Si/Carbon/Cmc Electrodes for Li-Ion Batteries. *Chem. Mater.* **2010,** 22, 1229-1241.
10. Komaba, S.; Shimomura, K.; Yabuuchi, N.; Ozeki, T.; Yui, H.; Konno, K., Study on Polymer Binders for High-Capacity Sio Negative Electrode of Li-Ion Batteries. *J Phys Chem C* **2011,** 115, 13487-13495.
11. Kwon, T. W.; Jeong, Y. K.; Lee, I.; Kim, T. S.; Choi, J. W.; Coskun, A., Systematic Molecular-Level Design of Binders Incorporating Meldrum's Acid for Silicon Anodes in Lithium Rechargeable Batteries. *Adv Mater* **2014,** 26, 7979-+.
12. Garsuch, R. R.; Le, D.-B.; Garsuch, A.; Li, J.; Wang, S.; Farooq, A.; Dahn, J. R., Studies of Lithium-Exchanged Nafion as an Electrode Binder for Alloy Negatives in Lithium-Ion Batteries. *J. Electrochem. Soc.* **2008,** 155, A721-A724.
13. Wu, M. Y.; Xiao, X. C.; Vukmirovic, N.; Xun, S. D.; Das, P. K.; Song, X. Y.; Olalde-Velasco, P.; Wang, D. D.; Weber, A. Z.; Wang, L. W.; Battaglia, V. S.; Yang, W. L.; Liu, G., Toward an Ideal Polymer Binder Design for High-Capacity Battery Anodes. *J Am Chem Soc* **2013,** 135, 12048-12056.
14. Kim, S. M.; Kim, M. H.; Choi, S. Y.; Lee, J. G.; Jang, J.; Lee, J. B.; Ryu, J. H.; Hwang, S. S.; Park, J. H.; Shin, K.; Kim, Y. G.; Oh, S. M., Poly(Phenanthrenequinone) as a Conductive Binder for Nano-Sized Silicon Negative Electrodes. *Energ Environ Sci* **2015,** 8, 1538-1543.
15. Liu, G.; Xun, S. D.; Vukmirovic, N.; Song, X. Y.; Olalde-Velasco, P.; Zheng, H. H.; Battaglia, V. S.; Wang, L. W.; Yang, W. L., Polymers with Tailored Electronic Structure for High Capacity Lithium Battery Electrodes. *Adv Mater* **2011,** 23, 4679-+.
16. Wu, H.; Yu, G. H.; Pan, L. J.; Liu, N. A.; McDowell, M. T.; Bao, Z. A.; Cui, Y., Stable Li-Ion Battery Anodes by in-Situ Polymerization of Conducting Hydrogel to Conformally Coat Silicon Nanoparticles. *Nat Commun* **2013,** 4.
17. Ryou, M. H.; Kim, J.; Lee, I.; Kim, S.; Jeong, Y. K.; Hong, S.; Ryu, J. H.; Kim, T. S.; Park, J. K.; Lee, H.; Choi, J. W., Mussel-Inspired Adhesive Binders for High-Performance Silicon Nanoparticle Anodes in Lithium-Ion Batteries. *Adv Mater* **2013,** 25, 1571-1576.

18. Jeong, Y. K.; Kwon, T.-w.; Lee, I.; Kim, T.-S.; Coskun, A.; Choi, J. W., Hyperbranched B-Cyclodextrin Polymer as an Effective Multidimensional Binder for Silicon Anodes in Lithium Rechargeable Batteries. *Nano Lett.* **2014,** 14, 864-870.
19. Jeong, Y. K.; Kwon, T. W.; Lee, I.; Kim, T. S.; Coskun, A.; Choi, J. W., Millipede-Inspired Structural Design Principle for High Performance Polysaccharide Binders in Silicon Anodes. *Energ Environ Sci* **2015,** 8, 1224-1230.
20. Ling, M.; Xu, Y. N.; Zhao, H.; Gu, X. X.; Qiu, J. X.; Li, S.; Wu, M. Y.; Song, X. Y.; Yan, C.; Liu, G.; Zhang, S. Q., Dual-Functional Gum Arabic Binder for Silicon Anodes in Lithium Ion Batteries. *Nano Energy* **2015,** 12, 178-185.
21. Wu, M. Y.; Sabisch, J. E. C.; Song, X. Y.; Minor, A. M.; Battaglia, V. S.; Liu, G., In Situ Formed Si Nanoparticle Network with Micron-Sized Si Particles for Lithium-Ion Battery Anodes. *Nano Lett* **2013,** 13, 5397-5402.
22. Choi, N. S.; Yew, K. H.; Choi, W. U.; Kim, S. S., Enhanced Electrochemical Properties of a Si-Based Anode Using an Electrochemically Active Polyamide Imide Binder. *J Power Sources* **2008,** 177, 590-594.
23. Koo, B.; Kim, H.; Cho, Y.; Lee, K. T.; Choi, N. S.; Cho, J., A Highly Cross-Linked Polymeric Binder for High-Performance Silicon Negative Electrodes in Lithium Ion Batteries. *Angew Chem Int Edit* **2012,** 51, 8762-8767.
24. Kovalenko, I.; Zdyrko, B.; Magasinski, A.; Hertzberg, B.; Milicev, Z.; Burtovyy, R.; Luzinov, I.; Yushin, G., A Major Constituent of Brown Algae for Use in High-Capacity Li-Ion Batteries. *Science* **2011,** 334, 75-79.
25. Liu, J.; Zhang, Q.; Wu, Z. Y.; Wu, J. H.; Li, J. T.; Huang, L.; Sun, S. G., A High-Performance Alginate Hydrogel Binder for the Si/C Anode of a Li-Ion Battery. *Chem Commun* **2014,** 50, 6386-6389.
26. Magasinski, A.; Zdyrko, B.; Kovalenko, I.; Hertzberg, B.; Burtovyy, R.; Huebner, C. F.; Fuller, T. F.; Luzinov, I.; Yushin, G., Toward Efficient Binders for Li-Ion Battery Si-Based Anodes: Polyacrylic Acid. *Acs Appl Mater Inter* **2010,** 2, 3004-3010.
27. Jeena, M. T.; Lee, J. I.; Kim, S. H.; Kim, C.; Kim, J. Y.; Park, S.; Ryu, J. H., Multifunctional Molecular Design as an Efficient Polymeric Binder for Silicon Anodes in Lithium-Ion Batteries. *Acs Appl Mater Inter* **2014,** 6, 18001-18007.
28. Ding, N.; Xu, J.; Yao, Y. X.; Wegner, G.; Lieberwirth, I.; Chen, C. H., Improvement of Cyclability of Si as Anode for Li-Ion Batteries. *J Power Sources* **2009,** 192, 644-651.